Available online at www.sciencedirect.com
ScienceDirect
Trans. Nonferrous Met. Soc. China 33(2023) 929−937
Transactions of Nonferrous Metals Society of China
www.tnmsc.cn

Influence mechanism of sucrose on phase change of K-feldspar during hydrothermal decomposition

Lai-shi LI[1], Jun-jie TANG[2], Yu-sheng WU[1], Meng YU[1]

1. School of Materials Science and Engineering, Shenyang University of Technology, Shenyang 110870, China;
2. School of Environmental and Chemical Engineering, Shenyang University of Technology, Shenyang 110870, China

Received 14 November 2021; accepted 1 May 2022

Abstract: Sucrose was added to the hydrothermal decomposition reaction of calcium oxide and K-feldspar to improve the adsorption performance of the hydrothermal product tobermorite. The effects of the sucrose concentrations on the decomposition rates of K-feldspar were studied based on the extraction rates of potassium oxide, and the influence mechanism of sucrose on the phase change of K-feldspar during the hydrothermal decomposition was elucidated. It was shown that when n(Su)/n(Ca)=0.1:1, the extraction rate of potassium oxide was 83.83%, and the decomposition of K-feldspar was inhibited with the increase of the sucrose concentration. The increase in the viscosity of the reaction system and the formation of calcium complexes during the hydrothermal process were the main reasons for the inhibition of the decomposition of K-feldspar. Moreover, the enhancement mechanism of the methylene blue adsorption capacity of the sucrose-modified tobermorite was explained from the perspective of the microstructure.
Key words: K-feldspar; sucrose; hydrothermal decomposition; adsorption; microstructure

1 Introduction

As a large agricultural country, China has a great demand for water-soluble potassium salts [1]. China is short of water-soluble potassium mineral resources, and the water-soluble potassium mineral resources that can be used to produce potash fertilizer are only 2.2% of the world's total reserves [2,3]. K-feldspar is composed of aluminum, silicon, potassium and oxygen in a stable tetrahedral network structure, which is hardly decomposed by acids and bases other than hydrofluoric acid at room temperature and pressure [4,5]. There are more than 60 exploration sources of potassium-rich rocks with K-feldspar as the main mineral phase in China, and the total reserves are more than 10 billion tons [6−8]. Therefore, it is of great research value and economic significance to study the efficient separation and extraction process of potassium in potash feldspar, which can make up for the shortage of soluble potassium salt resources in China.

The research on potassium extraction technology of K-feldspar has been paid attention to scholars at home and abroad. GAN et al [9] extracted water-soluble potassium salts from K-feldspar by an extraction process, reduced phosphogypsum to recover sulfur dioxide, and used the formed calcium compounds to reduce carbon dioxide emissions. But the treatment of industrial phosphogypsum consumes a large amount of energy, which has hindered its industrial application. LÜ et al [10] used 30% hydrofluoric acid to leach K-feldspar at 90 °C, and the extraction rate of potassium was 85.4%. This process produces a large amount of waste acid and causes serious

Corresponding author: Jun-jie TANG, Tel: +86-24-25496036, E-mail: tangjunjie1987@sut.edu.cn;
Yu-sheng WU, Tel: +86-24-25496300, E-mail: wuyus@sut.edu.cn
DOI: 10.1016/S1003-6326(23)66156-4
1003-6326/© 2023 The Nonferrous Metals Society of China. Published by Elsevier Ltd & Science Press

environmental pollution. Some scholars [11,12] believe that micro-organisms can disintegrate the lattices of K-feldspar, and this process involves chemical degradation to produce soluble potassium minerals, but the long degradation period makes this method unsuitable for industrial application.

Aiming at the deficiency of potassium extraction technology of K-feldspar, calcium oxide was used as restraining reagent to leach potassium from K-feldspar by a hydrothermal method. The advantage of this process lies in the new process of potassium extraction with no harmful gas generation, low energy consumption, and a high material utilization rate, which will effectively alleviate the shortage of potash fertilizer in China [13−15]. Related references show that the reaction of K-feldspar and calcium oxide at high temperatures produces tobermorite, hibschite, and other mineral compounds, as one of the hydrolysates of K-feldspar in this process, tobermorite is a good adsorption material [16−18]. As shown by the literature review above, scholars around the world have focused on the extraction rate of potassium, and there are few studies on the application of solid phase products after K-feldspar decomposition.

In this work, sucrose was added into the hydrothermal decomposition reaction of calcium oxide and K-feldspar to improve the adsorption performance of the hydrothermal product tobermorite. The liquid phase contained a soluble potassium salt, and a solid-phase product was used as a high-performance adsorption material to achieve the goal of zero discharge of process products. The influence of the sucrose concentration on the decomposition rate of K-feldspar was measured by the extraction rate of potassium oxide. XRD, SEM and Fourier-transform infrared spectroscopy (FTIR) were used to characterize the phases and morphologies of the solid phase hydrothermal products of K-feldspar under different sucrose concentrations, and the influence mechanism of sucrose on the phase change of K-feldspar during hydrothermal decomposition was elucidated. Moreover, the enhancement mechanism of the methylene blue adsorption capacity of the sucrose-modified tobermorite was explained from the perspective of the microstructure.

2 Experimental

2.1 Materials

The K-feldspar was from a mine in Tonghua city, Jilin Province, China, and its chemical composition is shown in Table 1. The K:Al:Si molar ratio was about 1:3:8, which is the theoretical composition of $KAlSi_3O_8$. The XRD pattern of the K-feldspar is shown in Fig. 1, and the XRD pattern indicates that the main crystal phase of K-feldspar is microcline with the chemical formula $KAlSi_3O_8$.. CaO, methylene blue, sucrose and all the other chemicals used in this study were of analytical grade and were purchased from National Pharmaceutical Group, China.

Table 1 Chemical composition of K-feldspar (wt.%)

SiO_2	Al_2O_3	K_2O	Fe_2O_3	Na_2O	MgO	Impurities
63.91	17.23	16.37	0.899	0.810	0.177	0.604

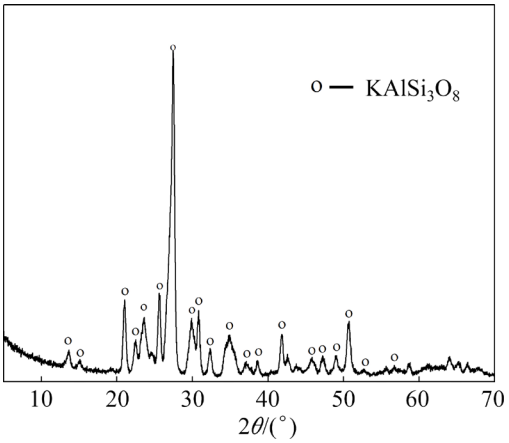

Fig. 1 XRD pattern of K-feldspar

2.2 Experimental procedure

The whole experimental process is shown in Fig. 2. Certain amounts of K-feldspar, deionized water, calcium oxide, and sucrose were inserted into the 150 mL steel projectiles, and the steel projectiles were fixed and heated in a hydrothermal heating reaction kettle. The hydrothermal temperature was 250 °C, the hydrothermal time was 8 h, the liquid to solid ratio was 20 mL/g, and the molar ratio of calcium to aluminum and silicon was 0.83:1:1. In the preliminary work, the decomposition rate of the K-feldspar under this hydrothermal condition was ideal. Therefore, this hydrothermal condition was selected. The molar

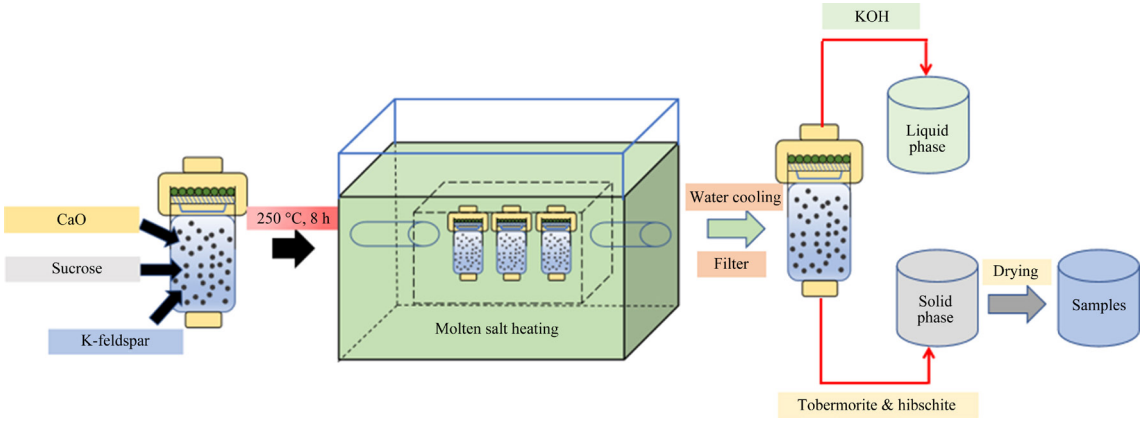

Fig. 2 Experimental flow chart

ratios of sucrose to calcium oxide were 0:1, 0.05:1, 0.1:1, 0.15:1, and 0.2:1. After the hydrothermal reaction, the hydrothermal reaction kettle was immediately placed in cold water for cooling, and the hydrothermal products were separated by vacuum filtration. The solid products obtained by vacuum filtration were washed with distilled water at 90 °C to a neutral pH. Then, the solid products after washing were dried in a drying oven at 105 °C. Above 120 °C, the crystalline water in the tobermorite and hibschite could be removed, so a drying temperature of 105 °C was selected. To investigate the effects of the sucrose concentration on the hydrothermal reaction of K-feldspar, the decomposition efficiency of K-feldspar was expressed by the extraction efficiency of potassium oxide.

The chemical reaction that has been involved in this experiment is as follows [19]:

$$4KAlSi_3O_8+13CaO+14H_2O=Ca_3Al_2(SiO_4)_2(OH)_4+2Ca_5Si_5AlO_{16.5}\cdot 5H_2O+4KOH \quad (1)$$

2.3 Analytical methods

The content of dissolved potassium in the solution was determined by inductively coupled plasma (ICP, Thermo, ICA-P6300 Radial). Solid hydrothermal products were characterized by X-ray diffraction (XRD, Shimadzu, XRD−7000). The light tube type was a Cu target, and ceramic X light tube. λ was 0.15406 nm, the scanning range was 10°−70°, and the scanning speed was 2 (°)/min. The chemical compositions of the hydrothermal products and the K-feldspar raw materials were determined by X-ray fluorescence spectroscopy (XRF, Thermo, ARL PERFORM X4200). In the SEM (SEM, Hitachi, SU 8010) tests, the electron acceleration voltage was 20.0 kV, the working distance was 21.8 mm, and the magnification was 15000 times. Fourier-transform infrared spectroscopy data were collected by the Bruker IF S66V spectrometer in the frequency range of 4000−400 cm^{-1} at the frequency step size of 4 cm^{-1}. The extraction efficient of K_2O in the experiments was defined as follows:

$$\eta = \frac{K/S - K/S_{residue}}{K/S} \quad (2)$$

where η is the extraction rate of K_2O (%), K/S is the mass ratio of K_2O to SiO_2 in the K-feldspar, $K/S_{residue}$ is the mass ratio of K_2O to SiO_2 in solid phase hydrothermal products.

3 Results and discussion

3.1 Effects of sucrose on hydrothermal decomposition products of K-feldspar

The influence of n(Su)/n(Ca) ratio on the extraction rate of K_2O is shown in Table 2. The extraction rate of K_2O was 84.47% without sucrose. When n(Su)/n(Ca)<0.10:1, the extraction rate of K_2O exhibited no change. However, when n(Su)/n(Ca)>0.10:1, the extraction rate of K_2O decreased significantly, and when n(Su)/n(Ca)= 0.20:1, the extraction rate of K_2O was 59.09%. These

Table 2 Extraction rates of K_2O at different n(Su)/n(Ca) ratios

n(Su)/n(Ca)	Extraction rate/%
0:1	84.47
0.05:1	84.25
0.10:1	83.83
0.15:1	69.39
0.20:1	59.09

results showed that sucrose had chemical activity in the hydrothermal system ($CaO-SiO_2-H_2O$) and had significant influence on the decomposition efficiency of K-feldspar.

The hydrothermal products under different n(Su)/n(Ca) ratios were characterized by XRD, as shown in Fig. 3. The mainly hydrothermal products were tobermorite, hibschite, and undecomposed K-feldspar. When n(Su)/n(Ca)=0.05:1, a fuzzy and wide peak of tobermorites appeared at $2\theta\approx29°$. When n(Su)/n(Ca)=0.10:1, the two characteristic peaks of the tobermorites were found at $2\theta\approx29°$. The diffraction peak of the (110) plane was observed, which proved that the tobermorites began to grow along the (110) crystal plane. Moreover, the sizes of the characteristic peaks of the tobermorites at $2\theta\approx8°$ increased significantly, which further proved that the appropriate concentration of sucrose was beneficial to the crystallization of tobermorites.

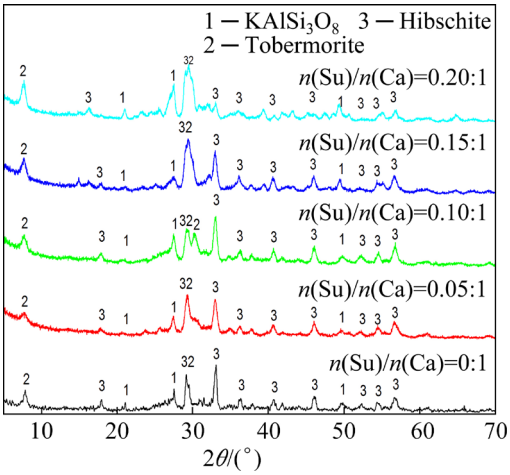

Fig. 3 XRD patterns of hydrothermal products with different n(Su)/n(Ca) ratios

When n(Su)/n(Ca)>0.1:1, the characteristic peak widths of the tobermorites at $2\theta\approx29°$ increased significantly, and one of the characteristic diffraction peaks of tobermorite disappeared. The results showed that the crystallinity of the tobermorites decreased significantly, and the excessive sucrose concentration was not conducive to the crystallization of tobermorites.

To investigate the effects of sucrose addition on the morphologies of the hydrothermal products, the hydrothermal products under different sucrose concentrations were characterized by SEM, as shown in Fig. 4. When no sucrose was added, the hydrothermal products were spherical tobermorites, and the small globular hibschites were attached to the surfaces of the tobermorites. The spherical tobermorites were composed of closely crossed needle-like crystals. When n(Su)/n(Ca)=0.1:1, the structures of the spherical tobermorites became loose. The surfaces of the spherical tobermorites were interwoven with layered crystals, and the small globular hibschites were attached to the surfaces. When n(Su)/n(Ca)=0.2:1, the incomplete decomposition of K-feldspar and the formation of tobermorites formed many small spherical aggregates. These aggregates were attached to the surfaces of a small number of spherical hibschites.

The above results showed that the addition of sucrose changed the morphology regularity of the hydrothermal products. The excessive sucrose concentrations inhibited the formation of tobermorites, which was consistent with the conclusion from the XRD that the crystallinity of the tobermorites decreased with the increase in the sucrose concentration. The addition of sucrose changed the structures of the tobermorites from compact to loose and porous ones, and the surface structures of the tobermorites also changed from closely crossed needle-like crystals to loose layered crystals. Relevant literature [20] showed that the surface morphology of tobermorites changed gradually from layered crystals to needle-like ones during the hydrothermal decomposition reaction of K-feldspar, and tobermorites coalesced to form xonotlites with the increase in the hydrothermal reaction time. In this study, the addition of sucrose changed the decomposition efficiency of the K-feldspar, which also slowed the crystallization efficiency of the tobermorites. Therefore, the tobermorites showed different morphologies, and no xonotlites formed.

To clarify the effects of the sucrose addition on the tobermorite contents in the hydrothermal products, the hydrothermal products under different sucrose concentrations were characterized by FTIR, as shown in Fig. 5. The FTIR spectra showed main narrow bands near 958 cm^{-1}, which were typical of the Si—O stretching vibrations generated by Q^2 silicon sites. The 1181 cm^{-1} bands were caused by the Si—O stretching vibrations in the Q^3 silicon sites of tobermorite. The bands at 670 cm^{-1} were caused by Si—O—Si stretching vibrations. The weak bands at 877 cm^{-1} were due to out-of-plane

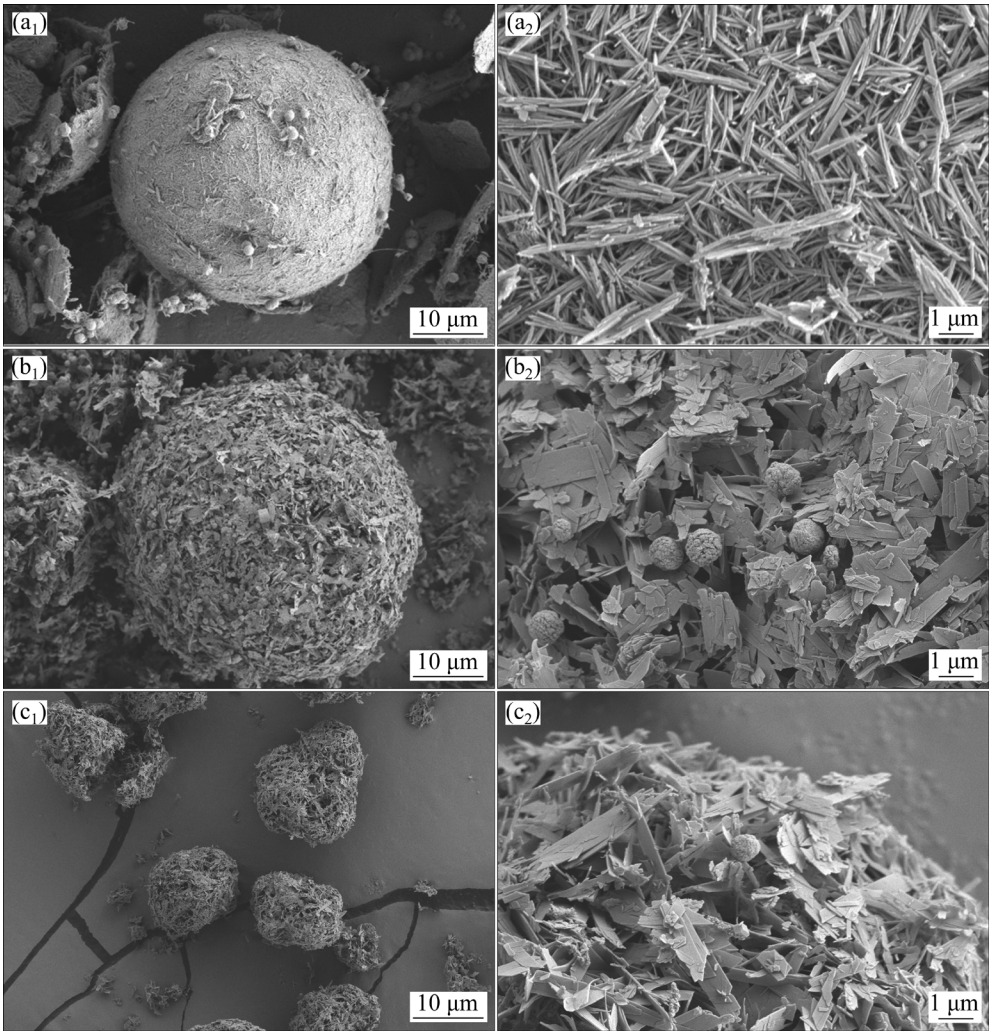

Fig. 4 SEM images of hydrothermal products under different sucrose concentrations: (a_1, a_2) n(Su)/n(Ca)=0:1; (b_1, b_2) n(Su)/n(Ca)=0.10:1; (c_1, c_2) n(Su)/n(Ca)=0.20:1

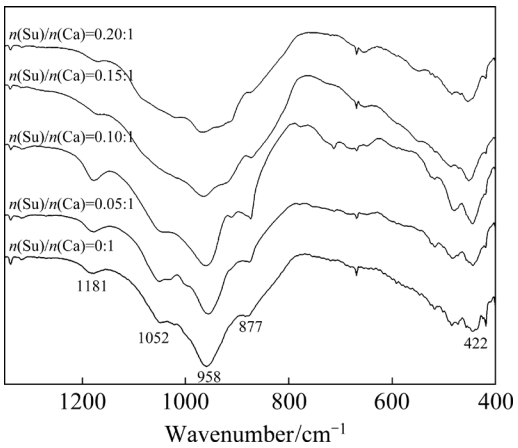

Fig. 5 FTIR spectra of hydrothermal products under different sucrose concentrations

bending of CO_3^{2-}. The generation of CO_3^{2-} may be related to sucrose degradation and CO_2 pollution during the hydrothermal reactions [21]. When n(Su)/n(Ca)=0.05:1 and 0.10:1, the peaks corresponding to Q^3 sites in the sample were clearer and stronger, indicating that there were more Q^3 sites in the samples and the tobermorite contents were higher. When n(Su)/n(Ca)=0.15:1 and 0.2:1, the peaks belonging to Q^3 sites almost disappeared at 1181 cm^{-1}. The peaks associated with Q^2 sites (958 cm^{-1}) became wide and weak, indicating that the polymerization degree of the silicate chains and the tobermorite contents were low.

3.2 Effect mechanism of sucrose on hydrothermal decomposition of K-feldspar

The pH after the hydrothermal reaction under different sucrose concentrations was determined. Because a large amount of potassium hydroxide was generated in the solution after the hydrothermal reaction, the solution pH was too high to be

measured by a pH meter. Therefore, the solution after the hydrothermal reaction was a constant volume to 500 mL, and then the pH was measured, as shown in Fig. 6.

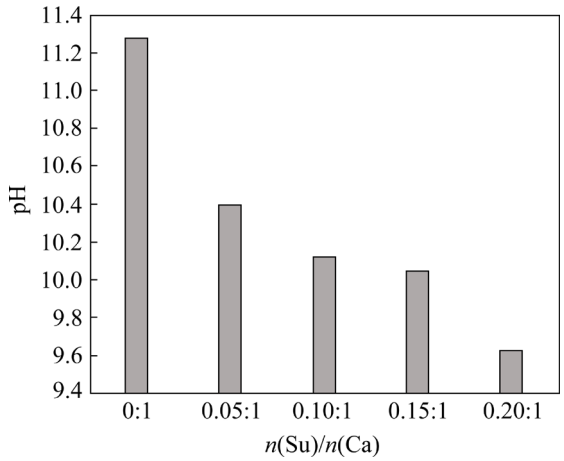

Fig. 6 pH before and after hydrothermal reaction under different sucrose concentrations

The pH remained unchanged at about 13.37 before the hydrothermal reaction. This indicated that sucrose did not react with K-feldspar and CaO at room temperature. However, with the increase in the sucrose concentration, the pH decreased gradually after the hydrothermal reaction. This was because the decomposition efficiency of the K-feldspar and the yield of KOH were reduced. Related literature showed that there were fixed relationships between the pH and Ca^{2+} concentration in the hydrolysis process of CaO [22]. The concentration of Ca^{2+} increased with the decrease in the pH in the range of 8−14 [23]. In this study, when n(Su)/n(Ca)>0.10:1, the decomposition rates of the K-feldspar decreased with the decrease in the pH values after the hydrothermal reactions. This shows that with the decrease in the pH, the Ca^{2+} decomposed from CaO did not react with the K-feldspar. In order to determine the reasons for this phenomenon, the absorbances of the solution after the hydrothermal reaction under different concentrations of sucrose were investigated, as shown in Fig. 7.

Relevant literature shows that sucrose is easily degraded by caramelization to form organic acids and polymers above 160 °C, and these organic acids usually include formic and acetic acids [24]. These substances are derived from the degradation of sucrose by caramelization at high temperatures [25]. An absorption peak centered at 290 nm appeared in the absorption spectrum of the reaction solution. This spike was thought to be caused by carbohydrates and organic acids, usually including formic and acetic acids [18]. When n(Su)/n(Ca)= 0.15:1 and 0.20:1, the absorbance of the solution increased significantly. This means that there were more caramelization intermediates in the solution. At the same time, these polymers increased the viscosity of the solution, as shown Fig. 8.

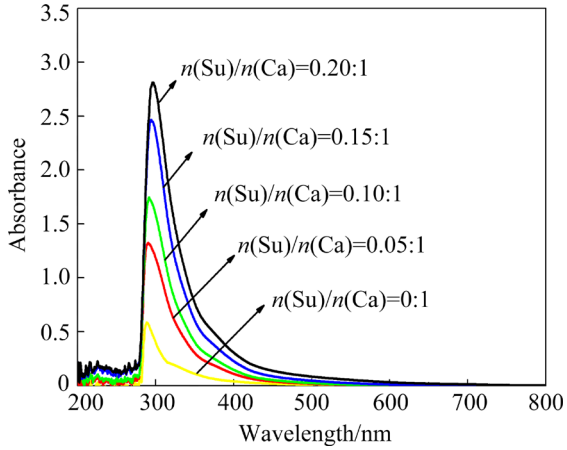

Fig. 7 Absorbance of solution after hydrothermal reaction

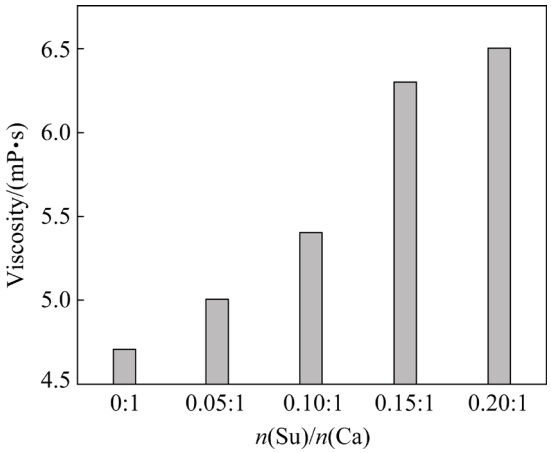

Fig. 8 Viscosity of solution after hydrothermal reaction under different concentrations of sucrose

The high viscosity solution had a blocking effect on the silicate materials. The increase in the solution viscosity inevitably reduced the ionic mobility, thus hindering the growth of diffusion-controlled calcium silicate hydrate [24]. Based on the results in Figs. 7 and 8, when n(Su)/n(Ca)=0.05:1 and 0.1:1, the concentrations of Ca^{2+} after the hydrothermal reactions were higher than those without sucrose. This was because sucrose and CaO in the hydrothermal reaction

process formed unstable complexes, which promoted the decomposition of CaO in the hydrothermal reaction process. These complexes hydrolyzed at high temperatures to Ca^{2+}. The Ca^{2+} obtained by hydrolysis compensated for the Ca^{2+} consumed in the hydrothermal reaction, which was beneficial to the forward hydrothermal reaction of K-feldspar and Ca^{2+}. This was also conducive to the growth of hydrothermal products tobermorite.

When n(Su)/n(Ca)=0.15:1 and 0.20:1, the excessive sucrose was complexed with Ca^{2+} to produce a large number of complexes, which reduced the effectiveness of Ca^{2+} in the hydrothermal reaction process. These complexes did not fully decompose into Ca^{2+} during the hydrothermal reaction to compensate for the consumption of Ca^{2+}. The formation of too many polymers consumed a large amount of Ca^{2+}. Although more CaO was dissolved in the solution, the amount of CaO reacting with the K-feldspar decreased. In addition, the high concentration of sucrose increased the viscosity of the solution and reduced the mobility of ions, which was not conducive to the hydrothermal reaction between K-feldspar and CaO. Based on these two factors, the hydrothermal reaction of K-feldspar with Ca^{2+} was hindered. Therefore, an excessive sucrose concentration was not conducive to the growth of tobermorite. The production of KOH decreased, resulting in a lower pH of the solution after the hydrothermal reaction. The above theoretical analysis was consistent with the SEM and XRD characterization of the tobermorites, which proved the accuracy of the theoretical analysis.

3.3 Effect of sucrose on adsorption properties of tobermorites

Methylene blue is widely used in chemical indicators, dyes, biological medicine, and other fields, but its aqueous solutions are toxic [26,27]. Therefore, the wastewater containing methylene blue must be discharged after harmless treatment. Tobermorite has certain adsorption properties for organic pigments such as methylene blue [28,29]. To study the effects of sucrose addition on the adsorption capacity of the tobermorites, an ultraviolet spectrophotometer was used to measure the absorbance values of the samples at a wavelength of 664 nm before and after adsorption. The absorbance was used to analyze the adsorption numerically. The adsorption amount of methylene blue on the tobermorites is expressed as [30]

$$Q_e=(C_0-C_e)V/m \quad (3)$$

where C_0 is the solution concentration of methylene blue before adsorption (mg/L), C_e is the solution concentration of methylene blue after adsorption (mg/L), V is the volume of methylene blue solution (L), and m is the adsorbent mass (g).

First, 0.1 g of hydrothermal products (tobermorites formed by hydrothermal reactions) were added to 50 mL of a 10 mg/L methylene blue solution. The influence of different adsorption time on the adsorption performance was analyzed, as shown in Fig. 9. During the adsorption process of methylene blue, the adsorption capacities of the two kinds of tobermorite samples increased sharply at first, and then slowed until the adsorption approached an equilibrium state (the adsorption time was 100 min). This was because there were many active points on the surface of the tobermorites at the beginning of the adsorption. However, with the

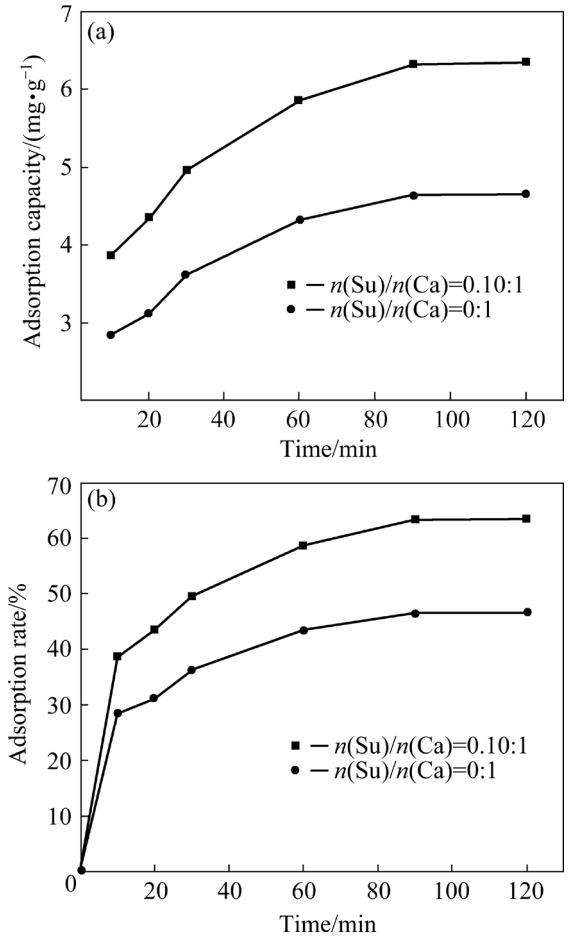

Fig. 9 Effect of adsorption time on adsorption capacity (a) and adsorption rate (b) of methylene blue

increase in the adsorption time, the active points on the surface were occupied, the adsorption rate decreased and finally reached an adsorption equilibrium state.

When the adsorption time was 100 min, the adsorption rate of the tobermorites prepared with n(Su)/n(Ca) of 0.10:1 was 63.5%. The adsorption rate increased by 16.9% compared to that of the sample without sucrose. This was because when the amount of sucrose was n(Su)/n(Ca)=0.10:1, the structure of the spherical tobermorites was loose. The surfaces of the spherical tobermorites were interwoven with layered crystals. The loose layered structure provided more surface active points, and the large gaps in the layered structure made it easier for methylene blue molecules to pass through the crystal surfaces. Therefore, the addition of sucrose-modified tobermorites yielded a better adsorption performance for methylene blue.

4 Conclusions

(1) The proper sucrose concentration was beneficial to the hydrothermal decomposition of K-feldspar by calcium oxide and the formation of tobermorite.

(2) The excessive sucrose complexed with Ca^{2+} to produce a large number of complexes. These complexes did not fully decompose into Ca^{2+} during the hydrothermal reaction to compensate for the consumption of Ca^{2+}, which was not beneficial to the hydrothermal decomposition of K-feldspar by calcium oxide and the formation of tobermorite.

(3) The excessive sucrose increased the viscosity of the solution and reduced the mobility of ions, which was not conducive to the hydrothermal reaction between K-feldspar and CaO.

(4) The morphology of the tobermorites changed from a closely crossed needle-like structure to a loose layered structure after adding sucrose, which enhanced the adsorption capacity of the tobermorites to methylene blue.

Acknowledgments

The present work was supported by the National Natural Science Foundation of China (No. 51974188), the Liaoning Revitalization Talents Program, China (Nos. XLYC2008014, XLYC1907080), the Young Teachers Research Ability Cultivation Fund of Shenyang University of Technology, China (No. QNPY202104), and the Key Research Project Fund of Shenyang University of Technology, China (No. X202167084).

References

[1] CICERI D, de OLIVEIRA M, CHEN D P, ALLANORE A. Role of processing temperature and time on the hydrothermal alteration of K-feldspar rock in autoclave [J]. Mining Metallurgy & Exploration, 2020, 37(4): 955−963.

[2] GUO Hui, KUANG Ge, LI Huan, PEI Wen-tao, WANG Hai-dong. Enhanced lithium leaching from lepidolite in continuous tubular reactor using H_2SO_4+H_2SiF_6 as lixiviant [J]. Transactions of Nonferrous Metals Society of China, 2021, 31(7): 2165−2173.

[3] SU Shuang-qing, MA Hong-wen, CHUAN Xiu-yun. Hydrothermal decomposition of K-feldspar in KOH−NaOH−H_2O medium [J]. Hydrometallurgy, 2015, 156: 47−52.

[4] CHENG Yong-sheng. Geochemistry of intrusive rock in Dachang tin-polymetallic ore field, Guangxi, China: Implications for petrogenesis and geodynamics [J]. Transactions of Nonferrous Metals Society of China, 2015, 25(1): 284−292.

[5] MA Jia-yu, DU Xue-lan, QIN Yuan-hang, WU Zai-kun, CHI Ru-an, WANG Cun-wen. Kinetics on leaching of potassium from phosphorus-potassium associated ore in HCl−H_3PO_4 media [J]. Transactions of Nonferrous Metals Society of China, 2017, 27(8): 1870−1877.

[6] MA Jia-yu, ZHANG Yan-fang, QIN Yuan-hang, WU Zai-ku, WANG Tie-lin, WANG Cun-wei. The leaching kinetics of K-feldspar in sulfuric acid with the aid of ultrasound [J]. Ultrasonics Sonochemistry, 2017, 35: 304−312.

[7] WANG Hong-tao. Study on the new technology of aluminum extraction from K-feldspar [D]. Shenyang: Shenyang University of Technology, 2018. (in Chinese)

[8] SONG Chao, ZHOU Yuan-yuan, LIU Quan-jun, DENG Jian-ying, LI Shi-mei, GAO Li-kun, YU Li. Effects of $BaCl_2$ on K-feldspar flotation using dodecyl amine chloride under natural pH [J]. Transactions of Nonferrous Metals Society of China, 2018, 28(11): 2335−2341.

[9] GAN Zhi-xin, CUI Zheng, YE Hai-rong, TANG Si-yang, LIU Chang-jun, LI Chun, LIANG Bin, XIE He-ping. An efficient methodology for utilization of K-feldspar and phosphogypsum with reduced energy consumption and CO_2 emissions [J]. Chinese Journal of Chemical Engineering, 2016, 24(11): 1541−1551.

[10] LÜ Li, LI Chun, ZHANG Guo-quan, HU Xiao-wei, LIANG Bin. Decomposition behavior of $CaSO_4$ during potassium extraction from a potash feldspar−$CaSO_4$ binary system by calcination [J]. Chinese Journal of Chemical Engineering, 2018, 26(4): 838−844.

[11] MOHAMMED S M O, BRANDT K, GRAY N D, WHITE M L, Manning D A C. Comparison of silicate minerals as sources of potassium for plant nutrition in sandy soil [J]. European Journal of Soil Science, 2014, 65(5): 653−662.

[12] BHATTACHARYA S, BACHANI P, JAIN D, PATIDAR S K, MISHRA S. Extraction of potassium from K-feldspar through potassium solubilization in the halophilic *Acinetobacter soli* (MTCC 5918) isolated from the experimental salt farm [J]. International Journal of Mineral Processing, 2016, 152: 53−57.

[13] HARTMANN A, BUHL J C. The influence of sucrose on the

crystallization behaviour in the system CaO−SiO−$C_{12}H_{22}O_{11}$−H_2O under hydrothermal conditions [J]. Materials Research Bulletin, 2010, 45(4): 396−402.
[14] ZHAO Jian-hai, LI Xi-lu, MENG Jiao, GE Wen-qi, LI Wen-pu. Microwave-assisted extraction of potassium from K-feldspar in the presence of NaOH and CaO at low temperature [J]. Environmental Earth Sciences, 2019, 78(9): 275.
[15] ZHANG Bai-yong, PAN Xiao-Lin, WANG Jiang-zhou, YU Hai-yan, TU Gan-feng. Reaction kinetics and mechanism of calcium oxide in dilute sodium aluminate solution with oxalate based on lime causticization [J]. Transactions of Nonferrous Metals Society of China, 2019, 29(6): 1312−1322.
[16] MA Xi, YANG Ji, MA Hong-wen, LIU Cang-jiang. Hydrothermal extraction of potassium from potassic quartz syenite and preparation of aluminum hydroxide [J]. International Journal of Mineral Processing, 2016, 147: 10−17.
[17] LIU Chun-li, MA Su-hua, DING Jian, LU Yang, ZHENG Shi-li, ZHANG Yi. Kinetics of decomposition of mullite and corundum in coal fly ash under highly alkaline condition [J]. Transactions of Nonferrous Metals Society of China, 2019, 29(4): 868−875.
[18] SU Shuang-qing, MA Hong-wen, CHUAN Xiu-yun, CAI Bi-ya. Preparation of potassium sulfate and zeolite NaA from K-feldspar by a novel hydrothermal process [J]. International Journal of Mineral Processing, 2016, 155: 130−135.
[19] QIU Mei-ya. Synthesis of tobermorite by dynamical decomposing potassium feldspar: An experimental study [D]. Beijing: China University of Geosciences, 2005. (in Chinese)
[20] LUO Zheng, MA Hou-wen, YANG Jing. Hydrothermal synthesis of acicular wollastonite from potassium silicate solution [J]. Journal of the Chinese Ceramic Society, 2017, 11(45): 1679−1685. (in Chinese)
[21] WANG Su-ping, PENG Xiao-qing, TANG Lu-ping, ZENG Lu, LAN Cong. Influence of inorganic admixtures on the 11Å-tobermorite formation prepared from steel slags: XRD and FTIR analysis [J]. Construction and Building Materials, 2014, 60: 42−47.
[22] TSUTSUMI T, NISHIMOTO S, KAMESHIMA Y, MIYAKE M. Hydrothermal preparation of tobermorite from blast furnace slag for Cs^+ and Sr^{2+} sorption [J]. Journal of Hazardous Materials, 2014, 266: 174−181.
[23] CAO Peng-xu, LI Guang-hui, LUO Jun, RAO Ming-jun, JIANG Hao, PENG Zhi-wei, JIANG Tao. Alkali-reinforced hydrothermal synthesis of lathy tobermorite fibers using mixture of coal fly ash and lime [J]. Construction and Building Materials, 2020, 238: 117655.
[24] ZHAO Zhi-guang, WEI Jiang-xiong, LI Fang-xian, YU Qi-jun. Study on the phase evolution of calcium oxide-silicon dioxide-water system incorporating sucrose under hydrothermal conditions [J]. Advances in Cement Research, 2017, 29(9): 359−372.
[25] JIANG Bin, LIU Ye-ting, BHANDARI B, ZHOU Wei-biao. Impact of caramelization on the glass transition temperature of several caramelized sugars. Part I: Chemical analyses [J]. Journal of Agricultural and Food Chemistry, 2008, 56(13): 5138−5147.
[26] GEORGIN J, FRANCO D S P, NETTO M S, ALLASIA D, OLIVEIRA M L S, DOTTO, G L. Treatment of water containing methylene by biosorption using Brazilian berry seeds (Eugenia uniflora) [J]. Environmental Science and Pollution Research, 2020, 27(17): 20831−20843.
[27] ALIM S A, RAO T S, MIDITANA S R, LAKSHMI K V D. Efficient and recyclable visible light-active nickel-phosphorus co-doped TiO_2 nanocatalysts for the abatement of methylene blue dye [J]. Journal of Nanostructure in Chemistry, 2020, 10(3): 211−226.
[28] DIAO Huai-ling, ZHANG Ze-jun, LIU Yun-xiao, SONG Zhong-qian, ZHOU Li-juan, DUAN Yong-xin, ZHANG Jian-ming. Facile fabrication of carboxylated cellulose nanocrystal-MnO_2 beads for high-efficiency removal of methylene blue [J]. Cellulose, 2020, 27(12): 7053−7066.
[29] MOHAMMADI S Z, MOFIDINASAB N, KARIMI M A, BEHESHTI A. Removal of methylene blue and Cd(II) by magnetic activated carbon–cobalt nanoparticles and its application to wastewater purification [J]. International Journal of Environmental Science and Technology, 2020, 17(12): 4815−4828.
[30] WANG Zhi-zeng, LI Tong, ZHAO Qin-yi, WANH Dong-yun, CUI Xiao-yi, CUI Cong. Adsorption of methylene blue by modified tobermorite [J]. Journal of the Chinese Ceramic Society, 2021, 49(06): 1185−1194. (in Chinese)

蔗糖对钾长石水热分解过程的相变影响机理

李来时[1]，唐俊杰[2]，吴玉胜[1]，于 猛[1]

1. 沈阳工业大学 材料与工程学院，沈阳 110870；2. 沈阳工业大学 环境与化学工程学院，沈阳 110870

摘 要：在氧化钙与钾长石的水热分解反应中加入蔗糖，以改善水热产物雪硅钙石的吸附性能。以氧化钾的提取率作为衡量标准，研究蔗糖浓度对钾长石分解速率的影响，阐明蔗糖对钾长石水热分解过程的相变影响机理。结果表明，当蔗糖与氧化钙的摩尔比为 0.1:1 时，氧化钾的提取率为 83.83%，随着蔗糖浓度的增加，钾长石的分解被抑制。反应体系黏度的增加和水热过程中钙络合物的形成是抑制钾长石分解的主要原因。此外，从微观形貌角度解释蔗糖改性雪硅钙石对亚甲基蓝吸附能力的增强机理。

关键词：钾长石；蔗糖；水热分解；吸附；微观形貌

(Edited by Xiang-qun LI)